

IRRADIATION TEST OF VACUUM CHAMBER FOR LANSCE ISOTOPE PRODUCTION FACILITY*

A.N.Drugakov, S.K.Esin, A.V.Feschenko, Yu.G.Kalinin, Yu.V.Kisselev, L.V.Kravchuk,
 A.N.Mirzozan, E.S.Nikulin, V.L.Serov (Institute for Nuclear Research, Moscow)
 M. Fagan, D. Ireland, K. F. Johnson, P. Walstrom (Los Alamos National Laboratory)

Abstract

Los Alamos National Laboratory is constructing a new Isotope Production Facility (IPF). IPF utilises a 100 MeV proton beam extracted from the transition region of the LANSCE accelerator by a kicker magnet. The vacuum chamber of the kicker must be fabricated from a material that is non-magnetic and non-conducting. Quartz was the material chosen for this application. However, the effect of a proton beam spill on the quartz chamber was not known. For this reason the chamber was irradiated with a proton beam that matched the beam conditions of the LANSCE transition region. The test has been done at the INR linac. The test equipment, the test procedure and the beam formation procedure are described and the experimental results are given.

1 INTRODUCTION

The tested prototype chamber fabricated from quartz is schematically shown in fig. 1.

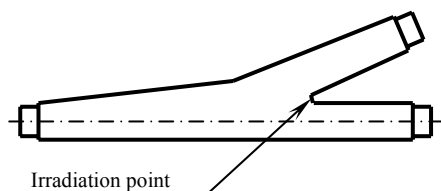


Figure 1: Sketch of the IPF prototype chamber.

According to the specification, the irradiation has to be done at the indicated in figure in the following sequence:

- Irradiation with a single pulse.
- If the chamber passes test "a", irradiation with ≥ 100 pulses.
- If the chamber passes the test "b", irradiation for 10 minutes or until destruction.

Beam parameter requirements:

- Proton energy – (100 ± 2) MeV.
- Pulse current – (16 ± 1) mA.
- Pulse duration – $50_{-0.0}^{+5.0}$ μ s.
- Repetition rate of beam pulses - 30 pulses/sec.
- Beam rms dimensions: $\sigma_x = 2.7 \pm 0.3$ mm,
 $\sigma_y = 1.5 \pm 0.3$ mm.

Preliminary analysis of the INR accelerator beam parameters and the accelerator geometry has shown that

the specified beam dimensions at the irradiation point can be more easily obtained for vertical rather than for horizontal installation of the chamber thus resulting in the interchange of X and Y notations below.

2 DESCRIPTION OF TEST EQUIPMENT AND TEST PROCEDURE

Test equipment is schematically shown in Fig. 2.

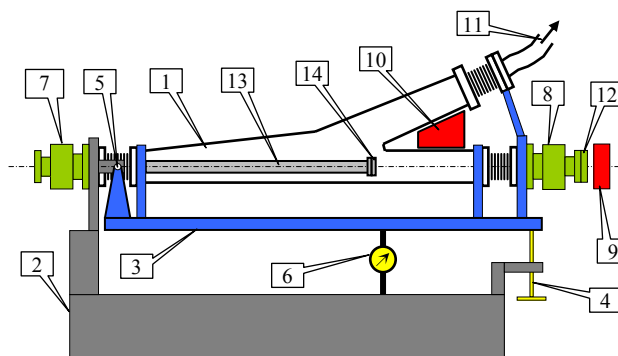


Figure 2: Schematics of test equipment (1-chamber, 2-unmovable frame, 3-moveable frame, 4-manual drive, 5-axis of rotation, 6- indicator of displacement, 7-wire scanner, 8- wire scanner, 9- beam dump, 10- water cooled beam dump, 11- vacuum pumping, 12- beam extraction window, 13- ion pipe and 14- beam extraction window).

The chamber was fixed to moveable frame 3. Two wire scanners, 7 and 8, were aligned with respect to the chamber axis. At first, a low repetition rate beam (1 pulse per second) was adjusted to obtain the specified beam dimensions and to fit the axis of the chamber. Then the beam was switched off and the moveable frame 3 was rotated with respect to axis 5 to locate the irradiation point on the beam axis. After that the beam repetition rate was increased up to 30 pulses/sec and the beam was turned on. During the irradiation the wires of the fixed wire scanner 7 were located in the beam and the corresponding signals were used to indicate beam position invariability. To protect the accelerator against possible vacuum breaks the vacuum volume of the chamber was separated from that of the accelerator by extraction window 14 (30- μ m aluminium foil positioned about 10 mm upstream of the irradiation point). Increases in the beam dimensions at the irradiation point due to scattering in the foil were negligible. The picture of the test equipment is given in fig. 3.

* Work supported by LANL under Agreement 31239-001-01-35.



Figure 3: Test equipment installed in beam line.

3 BEAM FORMING

The test equipment was installed in the 160 MeV intermediate extraction region of the INR linac. The beam was accelerated up to 100 MeV in the low energy part of accelerator and transported to the 160 MeV region without acceleration. The schematic diagram of the equipment used to form the beam is shown in Fig. 4.

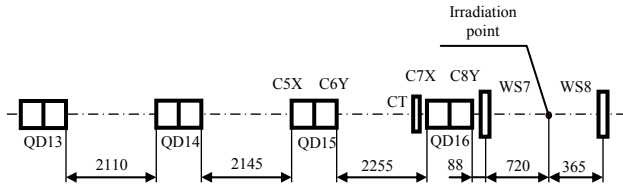


Figure 4: Schematic diagram of the equipment used to form the beam (QD13÷QD16 – quadrupole doublets; C5X,C7X – horizontal correctors; C6Y,C8Y – vertical correctors; CT – current transformer; WS7, WS8 – wire scanners 7 and 8 in fig. 2).

Beam forming included the following steps:

1. Forming of pulse current and pulse duration.
2. Measurement of beam emittance. The emittance was determined by measuring beam profiles with the wire scanner WS7 for different gradients in the doublets QD13÷QD16.
3. Calculation of beam optics and selection of the quadrupole gradients to obtain the specified beam dimensions at the irradiation point. Calculation of rms beam dimensions at wire scanners WS7 and WS8.
4. Beam steering to fit the chamber axis. Beam position and angle were measured with the wire scanners WS7 and WS8. The beam was steered with the correctors C5X, C7X, C6Y and C8Y.
5. Measurement the beam profiles using wire scanners WS7 and WS8. Comparing of the measured and the calculated (i. 3) rms beam parameters.

Figure 5 shows phase ellipses of the beam at the entrance of QD13. The straight lines represent $\pm\sigma$ boundaries of the beam at wire scanner WS7 transformed

to the entrance of QD13 for different QD13÷QD16 gradients within the region 680÷1320 Gs/cm (the corresponding currents 140÷280 A).

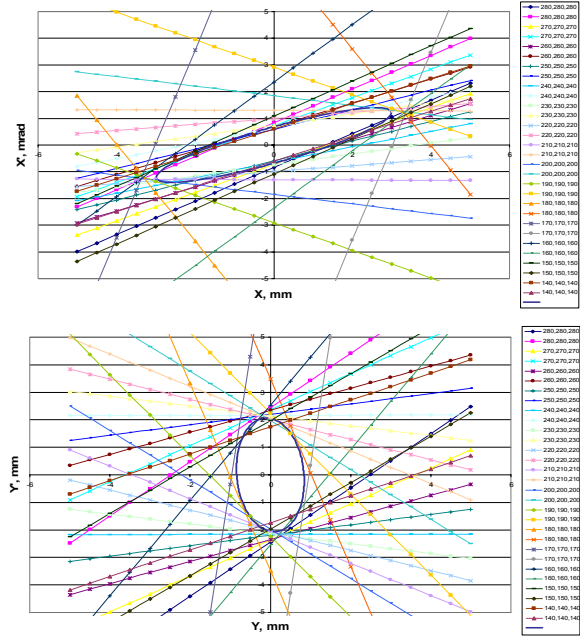


Figure 5: Beam phase ellipses at the entrance of QD13.

The ellipses and the rms beam dimensions found according to i.3 are given in Fig. 6 and Table 1.

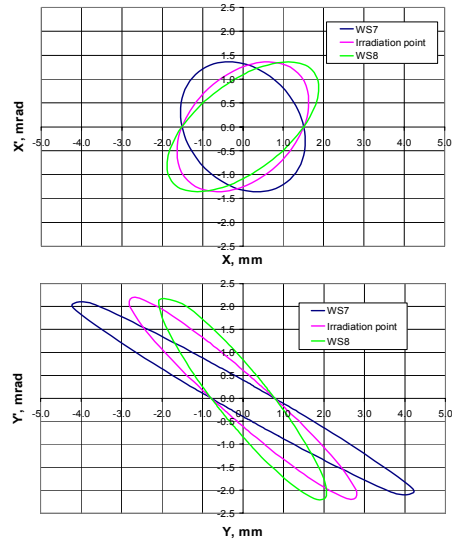


Figure 6: Beam phase ellipses at WS7, WS8 and the irradiation point.

Table 1: Calculated and measured rms beam dimensions

		σ_x , mm	σ_y , mm
WS7	calculated	1.55	4.37
	measured	1.67	4.01
Irradiation point	calculated	1.63	2.82
	measured	1.77	1.73
WS8	measured	1.77	1.73
	calculated	1.88	2.06

4 EXPERIMENTAL RESULTS

During irradiation the following parameters were monitored:

- Beam current.
- Signals from the wires of wire scanner WS7.
- Pressure inside the chamber.
- TV image of the irradiation point.

The chamber successfully passed tests “a” and “b”. The images observed during test “c” are shown in fig. 7.

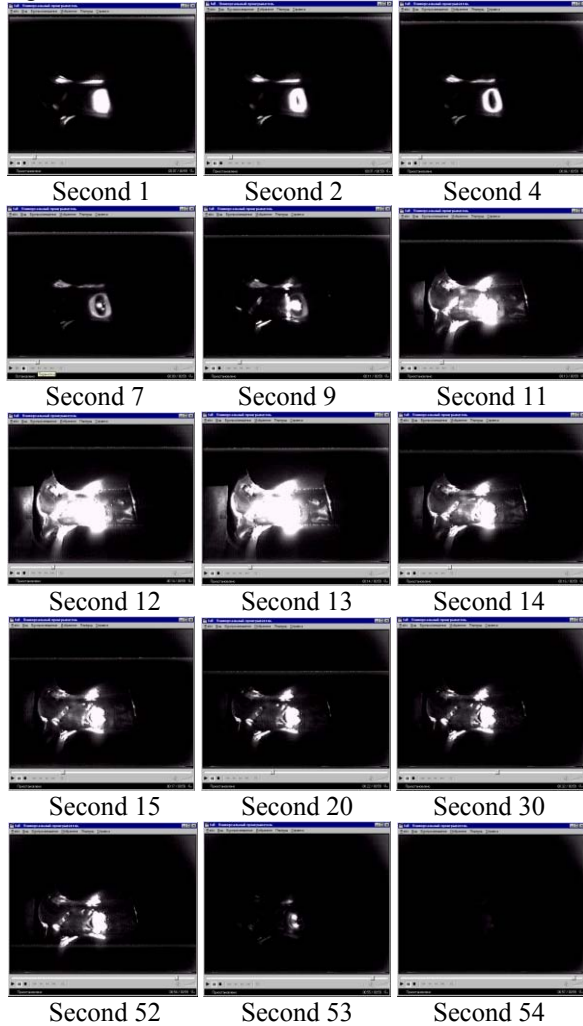


Figure 7: TV images during test “c”.

After about two seconds one can observe the appearance of a black spot in the beam centre. It can be explained by the non-uniform spectral sensitivity of the TV camera. Further heating resulted in an increase of the spot size. Temperature rise resulted in the occurrence of another spot, a white one, after the 6th ÷ 7th second. The size of the spot increases until the chamber wall is burned through at the end of the 13th second.

Vacuum inside the chamber was monitored with a Penning gauge. The pressure during the test was equal to about $6 \cdot 10^{-5}$ Pa. Changes in pressure during irradiation

due to beam impact or material heating were not observed. The signal from the vacuum detector was incorporated into the interlock system to switch off the beam. However, fast vacuum break at the end of the 13th second resulted in a malfunction of the vacuum detector. The interlock signal was not generated. As a result the beam was not interrupted and remained on for additional 39 seconds until it was switched off by an operator. During this additional time the TV picture was unchanged due to cooling of the impact point by air flow.

The picture of the chamber after the test is given in Fig. 8. The size of the burn hole was about 1 mm. Figure 9 demonstrates the 0.8 mm pin passing through the hole. The funnel at the inner side can be explained by air flow during the irradiation after the chamber wall had been burned through.

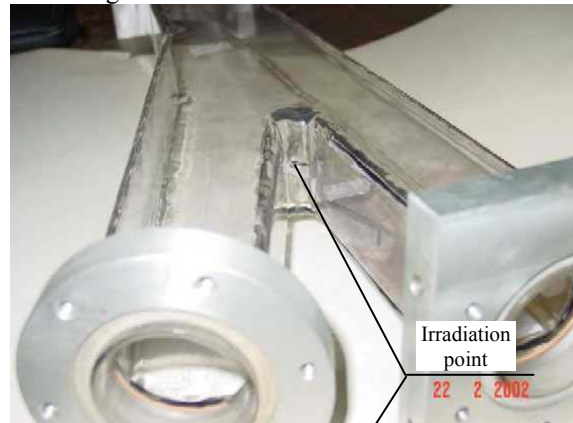


Figure 8: Chamber after irradiation test “c”.



Figure 9: Demonstration of the burned through hole with the 0.8-mm pin.

5 CONCLUSION

The chamber passed tests “a” (irradiation with a single pulse) and “b” (irradiation with 100 pulses). The chamber was burned through during the test “c” after 13 seconds. The size of the hole was about 1 mm. The tests have shown that the lifetime of the chamber is much longer than the protection system dead time and the quartz chamber can be successfully used to extract the beam to the IPF of the LANSCE accelerator.